Special Feature: Active Safety

Research Report

Angular Spread Estimation of Reflected Signal for Automotive Radar

Masaru Ogawa

Report received on Jan. 23, 2012

ABSTRACT A derivative constrained Capon estimator using an integrated mode vector (DECCIM) suitable for automotive radar is proposed. The DECCIM estimates the angular spread (AS) and direction-of-arrival (DOA) of a reflected signal composed of several element waves reflected simultaneously from an object. The method uses an integrated mode vector in which the AS is considered and includes within its constraint condition the derivative of the integrated mode vector. The estimation performance of the method is demonstrated via some numerical examples. When the element waves all have phases of 0 degrees and the SNR is greater than 20 dB, the estimation errors of the AS and DOA are less than 1.0 degree. The standard deviations of the AS and DOA are less than 1.5 degrees. In the case of a larger aperture sensor array, a lower SNR can be effectively estimated. Furthermore, when the phase of each element wave is given at random, the estimation errors of the AS and DOA are almost equivalent to the results obtained for a constant phase of 0 degrees. The potential of the DECCIM method for practical application is demonstrated.

KEYWORDS Automotive Radar, Reflected Signal, Angular Spread, Direction-of-arrival, Capon, Integrated Mode Vector, Derivative Constrained

1. Introduction

Recently, automotive radar has been studied and developed for use in ACC systems or collision mitigation systems.[1-4] An indispensable function of any radar system is to detect the relative range, velocity, and direction of an object. In collision mitigation or avoidance systems, it is additionally important to estimate the width of the detected object. The reflected signal which an automotive radar receives consists of element waves reflected from several different points on the object.[5] This is because the shape of the object is complex unlike a plane or a sphere.

Hence, multi- or scanning-beam radars with high resolution in the azimuth direction are proposed as a technique to estimate the width of an object.[6] These radars obtain several reflected waves as the object image. However, it may be difficult to obtain suitable signals from mounted vehicles even if the radars use super-resolution techniques such as MUSIC (Multiple Signal Classification) method.[7] To obtain high resolution the radars require a large array aperture with many sensors. In addition, the signal processing time will increase as the number of element waves increases.

We propose a derivative constrained Capon estimator using an integrated mode vector (DECCIM) as a suitable method for automotive radar, and demonstrate the performance of DECCIM via some numerical examples.[8] The DECCIM method estimates the angular spread (AS) and direction-of-arrival (DOA) of a reflected signal composed of several element waves reflected simultaneously from the object. In the Capon method [9] it is unnecessary to know the number of reflected waves, and its calculation cost is lower than other super-resolution methods. Furthermore, the constraint condition of the method can be extended easily. The DECCIM method utilizes an integrated mode vector in which AS is considered, and includes within the constraint condition the derivative of the integrated mode vector.

2. Problem Formulation

Figure 1 shows a model of the reflected signal and the uniform linear sensor array. Let us consider the reflected signal composed of M element waves reflected from an object, and an array comprising K sensors with a sensor spacing of d. Each element wave belonging to the reflected signal is fully correlated with the others. θ_m and A_m denote the DOA and complex amplitude of the m-th element wave, respectively. The AS and DOA of the reflected signal are represented by

$\Delta\theta$ and θ, respectively, that is

$$\Delta\theta = \theta_M - \theta_1,\ \theta = \frac{\theta_M + \theta_1}{2}\quad (\theta_1 < \theta_2 < \cdots < \theta_M). \cdots\cdots\cdots\cdots (1)$$

In this case, the array output vector $\mathbf{x}(t)$ in the presence of additive noise $\mathbf{n}(t)$ can be written as

$$\mathbf{x}(t) = \sum_{m=1}^{M} A_m \cdot \mathbf{a}_o(\theta_m) + \mathbf{n}(t), \cdots\cdots\cdots\cdots (2)$$

$$\mathbf{a}_o(\theta) = \left[a_{o1}(\theta), a_{o2}(\theta)\cdots, a_{oK}(\theta)\right]^T, \cdots\cdots\cdots (3)$$

$$a_{ok}(\theta) = \exp\left\{-j\frac{2\pi}{\lambda}d(k-1)\sin\theta\right\},\ (k = 1,2,\cdots, K) \cdots\cdots\cdots\cdots (4)$$

where $\mathbf{a}_o(\theta)$ and superscript T denote the mode vector of the array in the direction θ, and the transpose, respectively. It is assumed that the amplitude and phase are constant for the measurement duration due to a small snapshot number. When the several element waves are densely distributed, the summation in Eq. 2 is approximated by an integral equation, given as

$$\sum_{m=1}^{M} A_m \cdot \mathbf{a}_o(\theta_m) \cong s \cdot \int_{-\Delta\theta/2}^{\Delta\theta/2} V(\theta + z) \cdot \mathbf{a}_o(\theta + z) dz$$

$$s = \sum_{m=1}^{M} A_m,\ z = \theta_m - \theta \cdots\cdots\cdots\cdots (5)$$

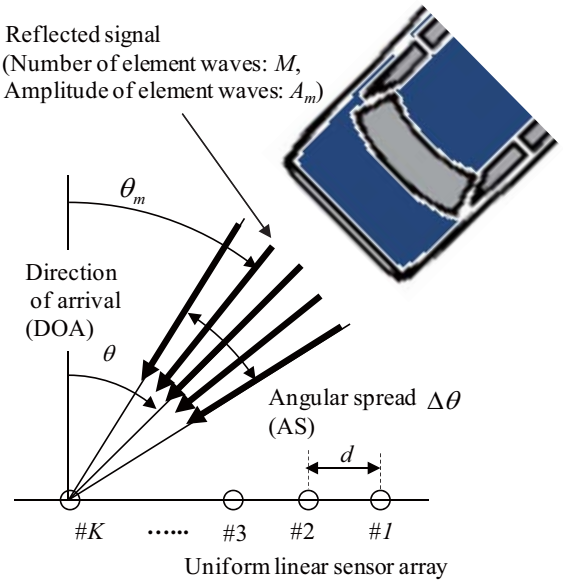

Fig. 1 Model of reflected signal and uniform linear sensor array.

where $V(z)$ is a function which expresses the complex amplitude distribution of the element waves in angle, while $V(z)$ satisfies

$$\int_{-\Delta\theta/2}^{\Delta\theta/2} V(z)\, dz = 1. \cdots\cdots\cdots\cdots (6)$$

Therefore, we make use of the following definition for the integrated array mode vector:

$$\mathbf{a}(\theta, \Delta\theta) = \left[a_1(\theta, \Delta\theta), a_2(\theta, \Delta\theta)\cdots, a_K(\theta, \Delta\theta)\right]^T \cdots\cdots\cdots\cdots (7)$$

$$a_k(\theta, \Delta\theta) = \int_{-\Delta\theta/2}^{\Delta\theta/2} V(\theta + z) \cdot a_{ok}(\theta + z)\, dz, \cdots\cdots (8)$$

where λ denotes the wavelength of the reflected signal and we assume the directional pattern of each sensor is omni-directional. Furthermore, when we assume $\Delta\theta \cong 0$ we obtain the following equation:

$$a_k(\theta, \Delta\theta) = a_{ok}(\theta) \cdot \int_{-\Delta\theta/2}^{\Delta\theta/2} V(\theta + z) \exp\left\{-j\frac{2\pi}{\lambda}d(k-1)z\cos\theta\right\} dz. \cdots\cdots\cdots\cdots (9)$$

Though we can define various functions for $V(z)$, we use here a raised triangular form, as shown in **Fig. 2**, in which the phase of $V(z)$ is 0 degrees (constant). This is because we take into account the amplitude distribution of the element waves as obtained by experimental results [5] and can execute the integral of Eq. 9 analytically. In Fig. 2, f_r is bounded by $0 \le f_r \le 1$.

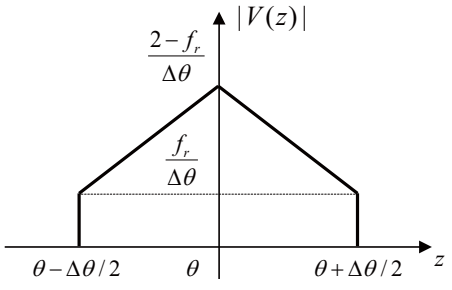

Fig. 2 Angular distribution of amplitude of $V(z)$. $(0 \le f_r \le 1)$

Hence,

$$a_k(\theta,\Delta\theta)=a_{ok}(\theta)\cdot\left\{(1-f_r)\cdot\mathrm{sinc}^2\left(\frac{uv}{2}\right)+f_r\cdot\mathrm{sinc}(uv)\right\},$$
$$u=\frac{2\pi}{\lambda}d(k-1)\cos\theta,\ v=\frac{\Delta\theta}{2} \quad \cdots\cdots\cdots\cdots (10)$$

Using the above definitions, the formulation of the DECCIM is described as follows:

$$\min\left(P_{out}=\frac{1}{2}\mathbf{w}^H R_{xx}\mathbf{w}\right)\ \text{subject to}\ C_{ig}^T\mathbf{w}^*=\mathbf{h}_{ig} \quad \cdots\cdots\cdots\cdots (11)$$

$$C_{ig}=\left[\mathbf{a}(\theta,\Delta\theta),\ \frac{\partial}{\partial\theta}\mathbf{a}(\theta,\Delta\theta)\right],\ \mathbf{h}_{ig}=[1,\ 0]^T \quad \cdots\cdots\cdots\cdots (12)$$

where superscript H and * denote the conjugate transpose and the conjugate, respectively. $\mathbf{w}$ is the weight vector and R_{xx} represents the covariance matrix of the array output vector $\mathbf{x}(t)$. P_{out} is the power of the combined output signal. The integrated mode vector $\mathbf{a}(\theta, \Delta\theta)$ is applied to the original Capon estimator. The constraint condition includes the derivative of $\mathbf{a}(\theta, \Delta\theta)$. The directivity of the sensor array at the constraint direction can be obtained at an extreme value by using the derivative of $\mathbf{a}(\theta, \Delta\theta)$. With this DECCIM, a null cannot be formed against element waves in the vicinity of the constraint direction. As a result, the DECCIM estimates the AS and DOA by finding the maximum values of the multidimensional spatial spectrum P_{deccim} with respect to θ and $\Delta\theta$:

$$P_{deccim}(\theta,\Delta\theta)=\mathbf{h}_{ig}^T(C_{ig}^H R_{xx}^{-1}C_{ig})^{-1}\mathbf{h}_{ig}^*. \quad \cdots\cdots\cdots (13)$$

The DECCIM performs poorly when coherent or highly correlated signals are present. In order to improve the estimation performance, forward/backward spatial smoothing processing (F/B SSP) [10] is applied to preprocess the array covariance matrix. Then, we obtain the smoothed covariance matrix

$$\overline{R_{xx}}=\frac{1}{2(K-K_s)}\sum_{K_s=1}^{K-K_s+1}\left[R_{xx}+R'_{xx}\right]_{K_s,k_s}, \quad \cdots\cdots (14)$$

where K_s and R'_{xx} denote the length of the subarray and the backward covariance matrix, respectively. In addition,

$$[B]_{K_s,k_s}=\begin{bmatrix} b_{k_s\ k_s} & \cdots & b_{k_s\ K_s+k_s-1} \\ \vdots & \ddots & \vdots \\ b_{K_s+k_s-1\ k_s} & \cdots & b_{K_s+k_s-1\ K_s+k_s-1}\end{bmatrix}, \quad \cdots\cdots\cdots\cdots (15)$$

where b_{ij} represents an element of the i-th row and j-th column of matrix B. The smoothed covariance matrix $\overline{R_{xx}}$ is used in Eqs. 11~13 instead of R_{xx}.

3. Simulation Results

For the simulations, a uniform linear array consisting of 12 sensors with half-wavelength sensor spacing is utilized. The parameters of the simulation are presented in **Table 1**. The amplitude distribution of the element waves is a raised triangle (f_r = 0.5 in Fig. 2), and the phases of all element waves are constant at 0 degrees. **Figure 3** shows the DECCIM spectrum, P_{deccim}, obtained from Eq. 13. The peaks of the spectrum indicate the estimated results for the AS and DOA of the detected reflected signal. As can be seen, the two reflected signals are detected separately. The estimated results for the AS and DOA are 3.2 degrees and 0.1 degrees, respectively, of the first signal and 6.0 degrees and 30.1 degrees, respectively, for the second signal.

Next, the basic performance is confirmed when the number of reflected signals is one. The true AS and

Table 1 Parameters used in simulation.

Number of sensors (K)	12
Sensor spacing (d)	0.5 wavelengths
Length of subarray (K_s)	6
Direction-of-arrival of #1	0 degrees
Angular spread of #1	3 degrees
Number of element waves of #1	10
SNR of #1	100 dB
Direction-of-arrival of #2	30 degrees
Angular spread of #2	6 degrees
Number of element waves of #2	15
SNR of #2	90 dB
Angular distribution of $\|V(z)\|$	f_r = 0.5
Phase of each element wave	0 degrees

DOA are 0 degrees and 3 degrees, respectively. The location of the sensor array and the angular distribution $V(z)$ are the same as given in Table 1. In addition, 100 independent trials were conducted to obtain the average and standard deviation for the AS and DOA estimates because thermal noise influences the accuracy of the estimation. The number of snapshots in each trial is one. **Figure 4** illustrates the average and standard deviation as a function of the signal-to-noise ratio (SNR). We define the estimation error as the difference between the true value and the average of the estimated result. Note that in the case of low noise the DECCIM method shows good performance. When the SNR is greater than 20 dB, the estimation errors for both the AS and DOA are less than 1.0 degree and the standard deviations are less than 1.5 degrees. When the SNR is 50 dB, the standard deviations of the AS and DOA are less than 0.2 degrees. On the other hand, **Fig. 5** shows the case in which the number of sensors K is 24, and the length of the subarray K_s is 12. It is easy to see that the estimation errors and standard deviations of the AS and DOA are improved when the noise level is high. When the SNR is 20 dB, the error and standard deviation are less than 0.3 degrees and 0.5 degrees, respectively. As a result, the DECCIM needs a larger array aperture to improve the estimation error and standard deviation of the AS and DOA. The array aperture is 12 wavelengths in Fig. 5.

Furthermore, we consider the case in which the phase of each element wave is given at random. **Figure 6** shows the simulation result as a function of the SNR of the reflected signal. The parameters of the simulation are the same as those in Fig. 4 with the

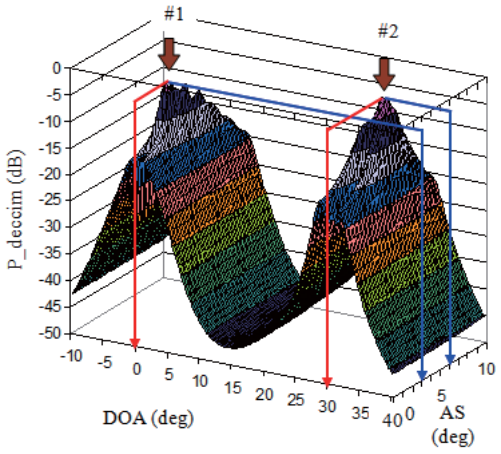

Fig. 3 Estimated results from DECCIM algorithm. Two signals are present in the field. The parameters of the simulation are shown in Table 1.

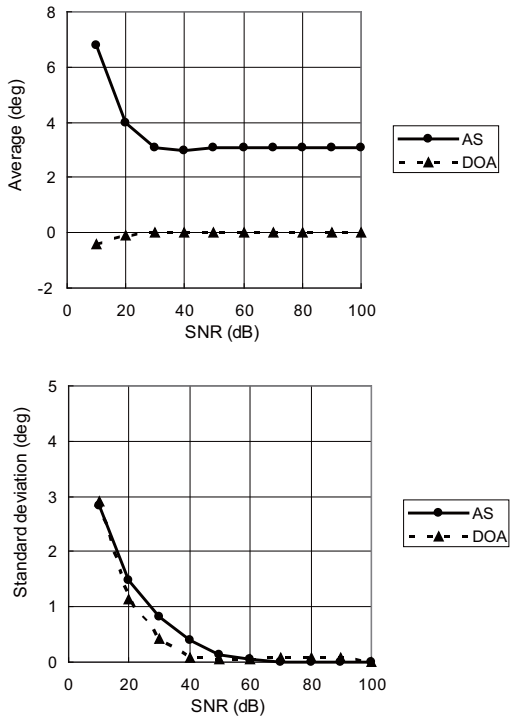

Fig. 4 Variation of the estimated AS and DOA with SNR. Parameters: number of sensors (K) = 12, phase of each element wave = 0 degrees, number of trials = 100.

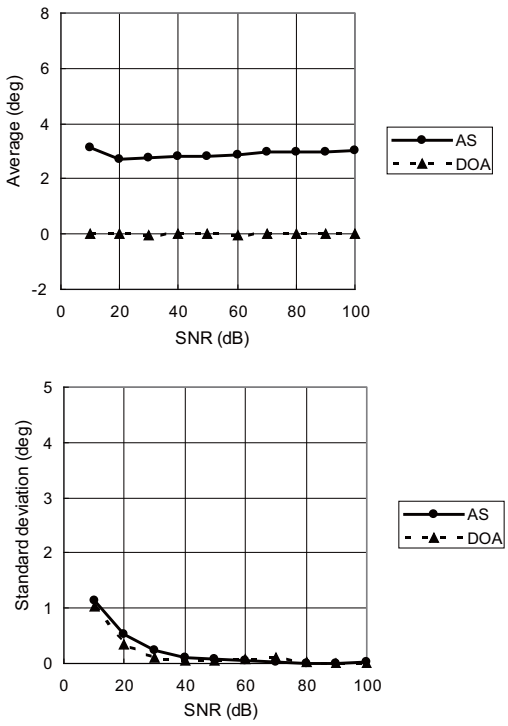

Fig. 5 Variation of the estimated AS and DOA with SNR. Parameters: number of sensors (K) = 24, phase of element waves = 0 degrees, number of trials = 100.

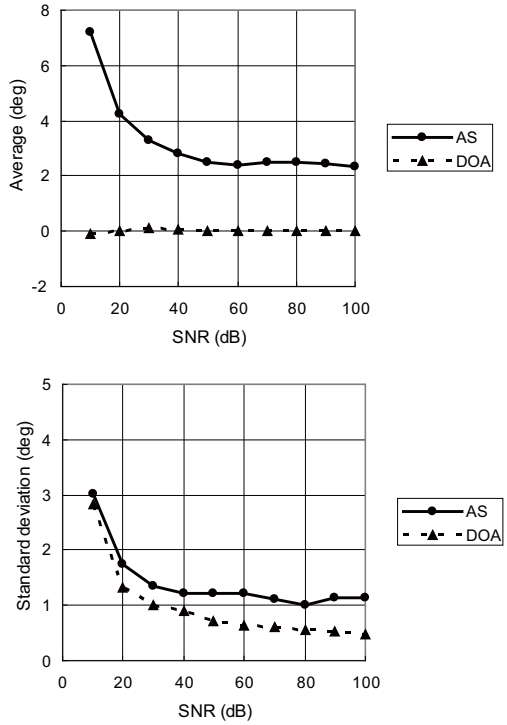

Fig. 6 Variation of the estimated AS and DOA with SNR. Parameters: number of sensors (K) = 12, phase of element waves is given at random, true AS = 3 degrees, true DOA = 0 degrees, number of trials = 1000.

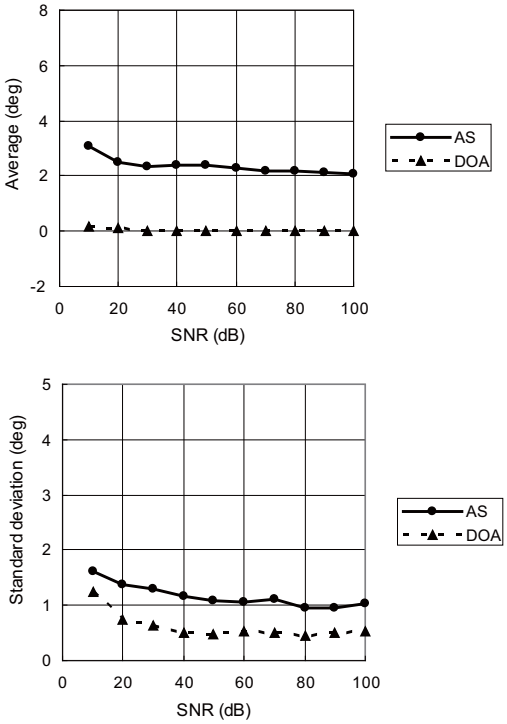

Fig. 8 Variation of estimated AS and DOA with SNR. Parameters: number of sensors (K) = 24, phase of element waves is given at random, true AS = 3 degrees, true DOA = 0 degrees, number of trials = 1000.

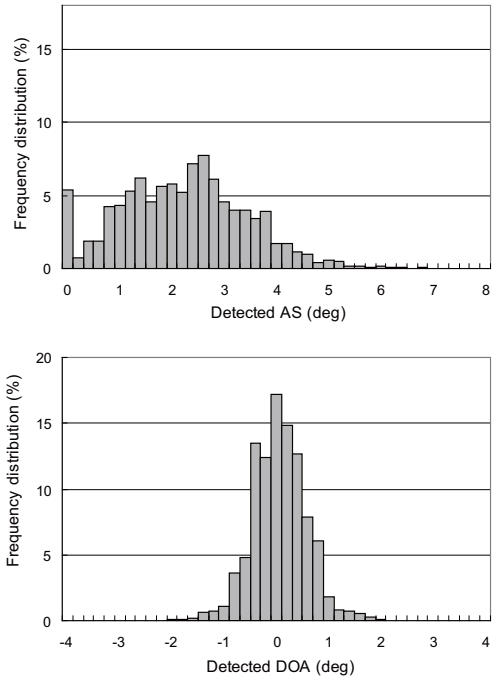

Fig. 7 Frequency distribution of estimated results in Fig. 6. Parameters: true AS = 3 degrees, true DOA = 0 degrees, number of trials = 1000.

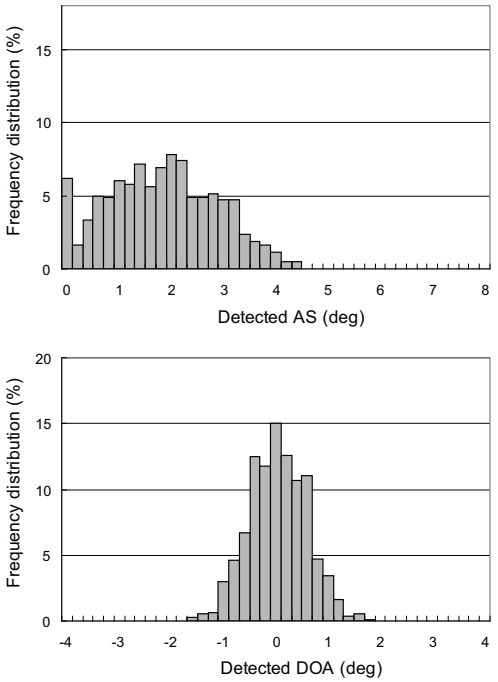

Fig. 9 Frequency distribution of estimated results in Fig. 8. Parameters: true AS = 3 degrees, true DOA = 0 degrees, number of trials = 1000.

exception of the phases of the element waves. The number of trials is 1000. The results shown in Fig. 6 indicate that the estimation errors of the AS and DOA are almost equal to those obtained in Fig. 4. However, the standard deviations of the AS and DOA deteriorate. For example, when the SNR is 50 dB, the standard deviations of the AS and DOA are 1.2 degrees and 0.7 degrees, respectively.

Figure 7 illustrates the frequency distribution of the estimated AS and DOA results in Fig. 6 when the SNR is 100 dB. Note that the frequency distribution peaks at around the true value. Consequently, the DECCIM method is robust to influences from the variance in phase of the element waves, as indicated by the average of the estimated AS and DOA values shown in Fig. 6, which are almost same as those in Fig. 4. This performance is important because the DECCIM method cannot determine the true phase of each element wave in the real environment. However, the DECCIM provides estimates which vary widely around the peak. In particular, the relative frequency at which the estimated AS is less than 0.2 degrees is 5.4%. It is significant to reduce this value in the next study.

Finally, **Fig. 8** shows the estimated results for the case in which the number of sensors K is 24 when the phase of each element wave is given at random. The parameters of the simulation are the same as those in Fig. 6 except for the number of sensors. In addition, **Fig. 9** represents the frequency distribution of the estimated results of the AS and DOA in Fig. 8 when the SNR is 100 dB. As a result, both the estimation errors and standard deviations of the AS and DOA are improved to the level obtained when the phase of each element wave was kept constant.

4. Conclusion

We have demonstrated that the DECCIM method can estimate the AS and DOA of a reflected signal composed of several element waves. When the phases of all element waves are constant at 0 degrees and the SNR is greater than 20 dB, the estimation errors of both the AS and DOA are less than 1.0 degree and the standard deviations are less than 1.5 degrees. In the case of a larger aperture sensor array, similar results can be obtained for a lower SNR. Furthermore, when the phase of each element wave is given at random, the estimation errors of the AS and DOA are almost equivalent to those obtained compared when the phase is kept constant at 0 degrees. These results demonstrate the practical potential of the DECCIM method in real-world applications.

References

(1) Asano, Y., Ohshima, S., Harada, T., Ogawa, M. and Nishikawa, K., “Proposal of Millimeter-wave Holographic Radar with Antenna Switching”, *IEEE MTT-S Int. Microw. Symp. Dig.* (2001), pp.1111-1114.
(2) Ogawa, M., Kidono, K. and Asano, Y., “Electrically Scanned Millimeter Wave Automotive Radar with Wide Detection Region”, *SAE 2003 World Congr.* (2003), *SAE Tech. Pap. Ser*. No.2003-01-0015.
(3) Tokoro, S., Kuroda, K., Kawakubo, A., Fujita, K. and Fujinami, H., “Electronically Scanned Millimeter Wave radar for Pre-crash Safety and Adaptive Cruise Control System”, *Proc. IEEE Intell. Veh. Symp.* (2003), pp.304-309.
(4) Ogawa, M., Asano, Y., Ohshima, S., Harada, T., Yamada, N., Watanabe, T. and Nishikawa, K., “Electrically Scanned Millimeter-wave Radar with Antenna Switching”, *Electron. and Commun. in Jpn.*, Part3, Vol.89, No.1 (2006), pp.10-20.
(5) Asano, Y., Ohshima, S. and Nishikawa, K., “Estimation of Received Signal Characteristics for Millimeter Wave Car Radar”, *IEICE Trans. Commun.*, Vol.E79-B, No.12 (1996), pp.1792-1798.
(6) Meis, U. and Schneider, R., “Radar Image Acquisition and Interpretation for Automotive Applications”, *IEEE Intell. Veh. Symp., Proc.* (2003), pp.328-332.
(7) Schmidt, O. R., “Multiple Emitter Location and Signal Parameter Estimation”, *IEEE Trans. Antennas & Propagat.*, Vol.AP-34, No.3 (1986), pp.276-280.
(8) Ogawa, M., Kikuma, N., Sato, K., Hirayama, H. and Sakakibara, K., “Derivative Constrained Capon Estimator Using Integrated Mode Vector”, *Proc. 5th Euro. Radar Conf.* (2008), pp.236-239.
(9) Capon, J., “High Resolution Frequency-wavenumber Spectrum Analysis,” *Proc. IEEE*, Vol.57 (1969), pp.1408-1418.
(10) Williams, T. R., Prasad, S., Mahalarabis, K. A. and Sibul, H. L., “An Improved Spatial Smoothing Technique for Bearing Estimation in a Multipath Environment,” *IEEE Trans. Acoust. Speech & Signal Process.*, Vol.36, No.4 (1988), pp.425-432.

Masaru Ogawa
Research Fields:
- Automotive Radar System
- Array Antenna and Signal Processing

Academic Degree: Dr. Eng.
Academic Society:
- The Institute of Electronics, Information and Communication Engineers